Available online at www.sciencedirect.com

SCIENCE DIRECT®

Journal of Catalysis 233 (2005) 257–265

JOURNAL OF CATALYSIS

www.elsevier.com/locate/jcat

Influence of adsorption parameters on catalytic cracking and catalyst decay

A. Corma [a,*], F.J. Ortega [a,b]

[a] *Instituto de Tecnología Química, UPV-CSIC, Universidad Politécnica de Valencia, Avda. de los Naranjos s/n, 46022 Valencia, Spain*
[b] *Instituto Mexicano del Petróleo, Eje Central Lázaro Cárdenas 152, 07730 México DF, Mexico*

Received 24 January 2005; revised 20 April 2005; accepted 21 April 2005

Abstract

Adsorption constants and heats of adsorption of different types of hydrocarbons on zeolitic catalysts have been obtained under cracking reaction conditions, by means of kinetic techniques. The heat of adsorption of a naphthene is very close to the alkane with the same number of carbon–carbon bonds, which in turn is defined by the van der Waals interactions between the hydrocarbon and the zeolite walls. The presence of the double bond in the olefin increases the heat of adsorption of the corresponding alkane by ∼40 kJ/mol. Comparison of decalin and tetralin shows the contribution of the aromatic ring to the heat of adsorption. Differences in heat of adsorption not only explain differences in cracking conversion, but can also predict variations in catalyst decay when industrial feeds of different compositions are used.

Keywords: Catalytic cracking; Kinetics; Hydrocarbon adsorption; Adsorption constants; Adsorption heats; Microactivity

1. Introduction

It is well known that adsorption of reactants on the catalyst surface is the first chemical step in a catalytic reaction. Adsorption is responsible for the preactivation of reactants, which results in a decrease of the activation energy of the process. It has been said, however, that in the case of catalytic cracking of alkanes with zeolites, the adsorption of the reactant corresponds to a van der Waals interaction between the alkane and the catalyst surface, and consequently the heat of adsorption is directly proportional to the number of carbons in the chain [1–4]. Then the apparent activation energy decreases when the number of carbon atoms in the reactant increases, but the true activation energy remains unchanged [5–8]. Babitz et al. found that when they cracked *n*-hexane over different zeolites (Y, mordenite, and ZSM-5), the apparent differences in activation energies are due to the different adsorption heats. Following these ideas, one could expect that the heat of adsorption of a long-chain olefin will have two components: one derived from the van der Waals interaction of the saturated part of the chain with the catalyst surface, and another, more localized, that may involve some electron transfer between the double bond and a Brønsted site of the catalyst. If this is so, a higher heat of adsorption for olefins than for paraffins would be expected. Likewise, hydrocarbon molecules containing aromatic groups should also have adsorption parameters different from those of either paraffins or olefins.

All this, which has its own interest from a fundamental point of view, for the rationalization of the adsorption interactions between solid catalyst and gaseous reactants, can also have important implications for the reaction of complex mixtures of molecules, since it occurs during catalytic cracking of industrial feeds. Indeed, in this case the feed or the partially cracked feed contains alkanes, alkenes, cycloalkanes, and aromatics. Thus, if one wishes to discuss feed reactivity, product selectivity, reaction kinetics, and catalyst decay, one should consider not only the differences in

---

[*] Corresponding author. Fax: +34 96 3877809.
E-mail address: acorma@itq.upv.es (A. Corma).

0021-9517/$ – see front matter © 2005 Elsevier Inc. All rights reserved.
doi:10.1016/j.jcat.2005.04.023

the intrinsic cracking rate of the group of molecules mentioned above, but also the differences in adsorption.

For instance, in the case of catalytic cracking, because of the lack of data, most authors make use of kinetic models that do not include adsorption parameters. However, adsorption and desorption parameters can play an important role in some cases [9]. Pruski et al. and Gianetto et al. have determined adsorption coefficients for gasoil and its lumped reaction products, showing the relevance of adsorption phenomena for catalytic cracking [10,11]. The same observations were made by Zhao and Wojciechowski when they cracked 2-methylpentane [12]; they also showed the impact of the heat of adsorption of reactants and products on catalyst decay. Bokhoven et al. used the Langmuir–Hinselwood formalism to show the dominant role of reactant sorption under conditions in which catalyst deactivation is considered negligible [13].

Although it is true that it is possible to carry out in situ adsorption measurements by means of techniques such as infrared spectroscopy, nuclear magnetic resonance, or calorimetric methods, among others, it is also true that such measurements are usually performed under conditions far from those under which the catalytic reactions occur.

Kinetic studies using pure compounds, on the other hand, can be used to determine adsorption parameters under reaction conditions. Kinetic equations may also provide valuable information on product adsorption and its effect on catalyst deactivation.

In the present work, we report results for cracking of some pure hydrocarbons (an alkane, an alkene, a cycloalkane, and an aromatic) over a commercial FCC catalyst containing USY zeolite. The corresponding kinetic and adsorption parameters of reactants and products were determined.

2. Experimental

2.1. Materials

1-Octene (Fluka; 99%), *cis–trans* decalin (Aldrich; >97%), and tetralin (Aldrich; >99%) were used as feedstocks without any further treatment.

A commercial low rare earth USY FCC catalyst (whose properties are listed in Table 1) was used to carry out the experimental work. Before the catalytic experiments, fresh catalyst was equilibrated by a steam treatment at 1089 K for 4 h with a mixture of 90 wt% steam and 10 wt% air. With this treatment the unit cell size of the zeolite in the catalyst was stabilized to 2.425 nm.

2.2. Experimental procedure

Experiments were performed in an automated computer-controlled micro activity test unit (MAT), which can carry out up to eight continuous experiments. Details of the apparatus and methodology have been described previously [14]. Each experiment consisted of a four-step cycle: stabilization, reaction, stripping, and regeneration. During the 30 min of the stabilization step, nitrogen is injected at a rate of 50 cc/min through the reactor, allowing temperatures to stabilize at the preset reaction temperature value. Before reaction, feed is pumped for 15 s into a purge collector to prevent any gas bubbles from entering the reactor. Then the feed is injected through the fixed-bed reactor and the reaction products are recovered in a cooled sampler. Liquid products are condensed in the sampler, and gases flow into an atmospheric burette, where they are accumulated for further analysis. After the reaction step, 100 cc/min of stripping nitrogen is fed through the catalytic bed for 15 min. Nitrogen sweeps liquid and gaseous hydrocarbons from the catalytic bed, and products are recovered in the cooled sampler and in the gas burette. To regenerate the deactivated catalyst, the coke produced by the reaction and deposited on the catalyst surface is burned off. Air is fed at a rate of 100 cc/min, and the flue gas from the reactor is sent into a catalytic furnace packed with copper oxides, where carbon monoxide is converted into carbon dioxide. After regeneration the catalyst is ready to start a new cycle.

Table 1
Catalyst properties

	Method	Fresh	Equilibrated
Bulk density (g/cc)	UOP-254	0.9	0.905
Specific area (m^2/g)	ASTM-D-3663	412	277
Zeolite specific area (m^2/g)	ASTM-D-3663	272	170
External specific area (m^2/g)	ASTM-D-3663	139	107
Pore volume (cc/g)	ASTM-D-4222	0.198	0.218
Unit cell size (Å)	ASTM 3942/80	24.49	24.25
Average particule size (μm)	ASTM-D-4464	70	70
Silica/alumina	–	6	60
Rare earths oxides (wt%)	IMP-QA-803	1	1

Thus, 3.0 g of equilibrated catalyst was loaded into the catalytic bed, and, after each set of experiments, the catalyst was discharged and characterized for a specific surface area and zeolite unit cell size. A bed of 3 cm of silicon carbide was placed above the catalyst bed as a preheater to ensure feed vaporization. A blank test was run for each hydrocarbon to measure thermal cracking, which resulted in less than 1.0 wt% at 773 K.

Conversion versus time on stream curves was built up in the range of 5–120 s while the feed flow and catalyst mass were kept constant. By doing this it was possible to observe the catalyst decay. To obtain data at different contact times, experiments were performed at different feed flows, 3.0, 4.0, and 5.0 g/min, respectively, over a catalyst mass of 3.0 g. Likewise, we monitored thermal effects by performing the experiments at two reaction temperatures, 673 and 773 K.

Catalyst stripping was done at reaction temperature with a flow of nitrogen at 100 ml/min, and catalyst regeneration was carried out at 813 K.

2.3. Product analysis

Gaseous products were analyzed with a Varian CX Chromatograph, equipped with a molecular sieve column, with argon as the carrier gas and a thermal conductivity detector to analyze H_2 and N_2. A plot alumina column with helium as the carrier gas and a flame ionization detector were used to analyze the hydrocarbons.

Liquid products were separated in a micro capillary column and analyzed by gas chromatography (Varian 3800). Conversion, which we followed by measuring the amount of reactant in products, was defined as the difference of reactant fed minus reactant content in products, which was equal to the sum of the gases, liquid products, and coke.

Coke was indirectly determined by measurement of the CO_2 from the regeneration flue gas with an infrared analyzer.

2.4. Kinetics

It is accepted that cracking catalyst deactivation occurs at such rapid rates that, for the rates of cracking to be properly quantified, the kinetics of conversion must be considered simultaneously with deactivation kinetics [15]. Thus, the kinetic equation that governs the experimental reactor has been derived by combining the mass balance of an ideal plug flow reactor, the reaction rate law, and the catalyst decay law:

$$\frac{\partial X}{\partial \tau} = \sum r_{A_i} \Phi, \tag{1}$$

where X is the instantaneous conversion of the reactant, τ is the feed space time, r_{A_i} is the reaction rate for each reaction, and Φ is the catalyst decay function.

To evaluate reaction rates, the following models were considered:

(a) the simple first-order pseudo-homogeneous rate law, which depends only on reactant concentration:

$$\frac{\partial X}{\partial \tau} = \sum Kr_i C_{A_0} \frac{(1-X)}{(1+\varepsilon X)} \Phi \tag{2}$$

and

(b) an equation based on the Langmuir–Hinselwood adsorption model, which includes the adsorption effects of reactants and products:

$$\begin{aligned}\frac{\partial X}{\partial \tau} = {} & \left(\sum Kr_i K_A C_{A_0} \frac{(1-X)}{(1+\varepsilon X)}\right) \\ & \bigg/ \left(1 + K_A C_{A_0} \frac{(1-X)}{(1+\varepsilon X)} \right. \\ & + \sum Kp_i n_i C_{A_0} X \frac{(1+\varepsilon)}{(1+\varepsilon X)} \\ & \left. + K_j \frac{C_{j0}}{(1+\varepsilon X)}\right) \Phi, \end{aligned} \tag{3}$$

where Kr_i is the reaction rate constant for each reaction, C_{A_0} is the initial concentration of reactant, C_{j0} is the initial inert concentration, ε is the volumetric expansion coefficient, K_A is the reactant adsorption constant, K_j is the inert adsorption constant, and $\sum Kp_i n_i$ is the term accounting for product adsorption and stoichiometry.

For catalyst deactivation, a second-order decay law based on time-on-stream theory was considered [16]:

$$\Phi = (1 + G t_f)^{-1}, \tag{4}$$

where G is the catalyst decay rate and t_f is time on stream.

These equations account for all reactions (cracking, isomerization, cyclization, etc.) through which the pure reactants are transformed into products and describe the evolution of instantaneous conversion as a function of space velocity, time on stream, and dilution ratio.

Because of catalyst decay, instantaneous conversion decreases as time on stream increases; thus the reported experimental conversion is the average of the cumulative instantaneous conversions during the experiment.

We obtained kinetic and adsorption parameters by fitting experimental conversion data to the above equations; we did this by comparing experimental and calculated conversions. To do this, we obtained the calculated conversion by averaging the instantaneous conversion from time $t_f = 0$ to time $t_f = T_f$, according to the expression

$$\overline{X} = \frac{1}{T_f} \int_0^{T_f} X \, dt_f, \tag{5}$$

where $\overline{X}$ is the average conversion, which corresponds to products accumulated from time zero to time T_f (final time on stream), X is the instantaneous conversion from Eqs. (2) and (3), and t_f is the time on stream.

To obtain the best fit of the experimental data, we optimized the values of the parameters by solving the above equations, coupled with the Buzzi optimization algorithm [17].

3. Results and discussion

1-Octene is mainly cracked into shorter (C_3–C_5) olefins; however, it is also transformed into other products by isomerization, hydrogen transfer, cyclization and oligomerization reactions. Products are also transformed by these reactions; for example, C_3–C_5 olefins are transformed into C_3–C_5 paraffins by hydrogen transfer.

At 673 K (Table 2) selectivity for cracking products was more than 30%, and hydrogen transfer was the second most important reaction, as indicated by the selectivity (>25%) for C_8 paraffins. Cyclization was also relevant; the selectivity for C_8 naphthenes was higher than 10%. Oligomerization (dimerization) also occurred to a significant extent; more than 10 wt% of 1-octane was transformed into heavier hydrocarbons. At 773 K (Table 3) 1-octene is almost completely transformed, selectivity for cracking products was

Table 2
Products selectivity at 673 K

	n-Hexadecane		1-Octene		Decalin		Tetralin	
TOS (s)	10	30	10	30	10	30	10	30
$C_1 + C_2$	0.16	0.11	0.26	0.08	0.18	0.13	1.75	2.46
Propane	1.55	1.06	0.21	0.05	0.86	0.41	0.99	0.68
Propylene	4.82	3.52	5.54	2.82	0.94	0.71	1.19	1.02
Butanes	10.53	7.16	4.72	0.79	4.13	2.96	2.97	2.56
Butenes	8.26	6.46	11.57	6.41	0.82	0.49	0.89	0.75
C_5 paraffins	14.54	11.70	3.76	0.67	1.34	1.23	1.78	1.71
C_5 olefins	6.17	6.02	6.77	4.50	0.41	0.18	0.30	0.34
C_5 naphthenes	0.00	0.00	0.00	0.00	0.00	0.07	0.00	0.00
C_6 paraffins	5.27	6.79	2.49	0.57	1.48	1.26	2.28	1.69
C_6 olefins	5.86	6.53	0.42	2.10	1.42	1.10	2.28	1.81
C_6 naphthenes	0.07	0.23	0.01	0.11	1.54	1.81	0.26	0.65
Benzene	0.06	0.03	0.02	0.03	0.01	0.02	4.38	6.97
C_7 paraffins	2.37	6.01	2.96	6.37	0.18	0.16	0.11	0.23
C_7 olefins	0.48	1.56	0.94	1.78	0.04	0.04	0.06	0.18
C_7 naphthenes	0.55	1.17	1.57	1.21	1.34	1.34	0.69	0.92
Toluene	0.63	0.25	1.02	3.27	0.21	0.15	2.52	3.31
C_8 paraffins	3.79	5.07	25.05	28.45	0.10	0.08	0.26	0.18
C_8 olefins	0.23	0.63	0.00	0.00	0.50	0.37	0.05	0.12
C_8 naphthenes	1.02	1.56	10.84	23.20	0.81	0.74	0.30	0.07
C_8 aromatics	0.88	0.88	1.95	1.07	1.10	1.23	2.77	3.25
C_9 paraffins	3.37	3.34	1.58	3.55	0.74	0.62	0.17	0.45
C_9 olefins	0.27	0.34	0.17	0.23	0.02	0.20	0.09	0.08
C_9 naphthenes	1.01	1.35	1.48	3.45	5.77	4.91	0.14	0.12
C_9 aromatics	1.32	0.75	1.88	0.99	9.72	4.59	2.34	2.75
C_{10} paraffins	1.52	1.56	0.83	0.45	10.20	11.10	2.02	1.66
C_{10} olefins	0.02	0.02	0.01	0.03	0.02	0.01	0.00	0.08
C_{10} naphthenes	1.70	1.27	0.25	0.20	7.30	10.30	1.48	1.18
C_{10} aromatics	0.88	1.73	2.83	1.48	31.59	39.49	9.60	10.50
C_{11} paraffins	0.69	0.62	0.09	0.02	0.47	0.46	0.30	0.60
C_{11} olefins	0.02	0.03	0.02	0.02	0.02	0.02	0.15	0.00
C_{11} naphthenes	0.03	0.04	0.01	0.02	0.60	0.85	0.23	0.27
C_{11} aromatics	1.43	1.56	0.65	0.45	2.91	3.65	6.61	3.86
C_{12+} paraffins	12.43	14.54	4.01	2.99	0.01	0.02	0.06	4.54
C_{12+} olefins	0.50	0.24	0.22	0.17	0.01	0.02	0.07	1.78
C_{12+} naphthenes	0.01	0.09	0.03	0.02	0.02	0.02	0.00	0.00
C_{12+} aromatics	1.80	2.60	0.70	0.32	2.80	3.20	5.68	14.48
Coke	5.38	3.08	4.47	3.10	10.32	6.38	45.42	29.01

Table 3
Products selectivity at 773 K

	n-Hexadecane		1-Octene		Decalin		Tetralin	
TOS (s)	10	30	10	30	10	30	10	30
$C_1 + C_2$	0.78	0.39	0.67	0.52	0.70	0.31	1.63	1.21
Propane	2.96	2.22	0.53	0.44	2.12	1.04	4.32	2.77
Propylene	10.00	7.98	13.00	12.13	3.93	1.85	4.32	2.77
Butanes	14.53	10.86	6.85	5.29	14.52	7.39	9.67	6.24
Butenes	23.74	20.58	25.15	24.07	2.91	1.52	2.96	2.09
C_5 paraffins	11.88	9.15	5.06	3.71	6.81	3.46	3.77	2.49
C_5 olefins	8.31	8.61	11.63	11.71	0.97	0.58	0.51	0.38
C_5 naphthenes	0.00	0.00	0.00	0.00	0.04	0.26	0.00	0.00
C_6 paraffins	5.30	5.80	2.03	1.67	4.46	2.82	3.49	1.48
C_6 olefins	6.30	6.08	1.42	2.33	4.31	2.02	3.73	1.44
C_6 naphthenes	0.03	0.19	0.08	0.11	3.46	5.68	1.15	1.32
Benzene	0.00	0.03	0.01	0.02	0.19	0.17	8.95	12.57
C_7 paraffins	1.18	4.14	1.08	1.22	0.48	0.62	0.25	0.30
C_7 olefins	0.29	1.11	0.72	1.08	0.04	0.04	0.13	0.15
C_7 naphthenes	0.26	0.69	1.05	1.22	4.10	4.94	0.76	1.00
Toluene	0.22	0.27	0.44	0.59	1.58	1.14	4.21	6.59
C_8 paraffins	1.69	3.85	12.87	15.50	0.38	0.45	0.17	0.22
C_8 olefins	0.09	0.17	0.71	0.92	0.03	0.05	0.02	0.03
C_8 naphthenes	0.43	0.80	1.94	2.56	9.55	12.85	0.17	0.26
C_8 aromatics	1.12	1.00	3.10	3.11	2.11	1.60	2.63	4.15
C_9 paraffins	1.31	1.72	0.58	0.76	1.50	1.53	0.26	0.45
C_9 olefins	0.11	0.18	0.03	0.04	0.38	0.51	0.03	0.03
C_9 naphthenes	0.36	0.60	0.38	0.59	3.92	7.38	0.21	0.33
C_9 aromatics	0.62	0.63	2.38	2.30	3.46	4.43	2.56	3.30
C_{10} paraffins	0.80	0.79	0.30	0.15	6.14	8.35	1.86	2.25
C_{10} olefins	0.01	0.08	0.01	0.01	0.07	0.13	0.03	0.18
C_{10} naphthenes	0.10	0.10	0.05	0.05	0.20	0.32	0.72	0.91
C_{10} aromatics	0.73	1.82	2.54	2.39	10.48	15.51	7.25	18.84
C_{11} paraffins	0.11	0.37	0.03	0.03	0.49	0.51	0.13	0.14
C_{11} olefins	0.00	0.01	0.00	0.00	0.00	0.01	0.00	0.00
C_{11} naphthenes	0.01	0.00	0.00	0.00	0.00	0.00	0.75	1.14
C_{11} aromatics	0.21	0.20	0.43	0.43	2.48	3.94	8.12	13.79
C_{12+} paraffins	2.30	5.56	2.70	2.43	0.02	0.10	1.60	1.86
C_{12+} olefins	0.03	0.04	0.13	0.13	0.01	0.09	0.39	0.21
C_{12+} naphthenes	0.00	0.01	0.01	0.01	0.02	0.02	0.00	0.00
C_{12+} aromatics	0.14	2.30	0.35	0.32	3.30	1.66	7.86	2.88
Coke	3.78	1.61	1.66	1.32	4.75	6.56	15.38	6.26

higher than 65%, hydrogen transfer was lower than 15%, and selectivity for cyclization and oligomerization was less than 10%.

It has been reported [18] that decalin is transformed by the opening of the naphthenic rings, yielding an olefin-substituted naphthene, which reacts by hydrogen transfer to produce aromatics and a paraffin-substituted naphthene. Cracking of the side chain of the substituted naphthene produces propylene and butylenes that are also transformed into the corresponding paraffins by hydrogen transfer. At 673 K (Table 2) more than 30% of decalin is transformed into aromatic hydrocarbons by hydrogen transfer; cracking of the substituted naphthenes occurs at a lower extent, as indicated by the low selectivity for propane and butanes. At 773 K cracking increases considerably, but hydrogen transfer reactions still occur (Table 3). Hydrogen transfer has been shown to depend on acid site density regardless of whether the catalyst contains rare earth cations [19].

Tetralin is also transformed by the opening of the naphthenic ring, which leads to the formation of C_2–C_4 alkenyl aromatics, which in turn are converted by hydrogen transfer into alkyl aromatics, naphthalene and other aromatics, and coke. At 673 K the selectivity for hydrogen transfer products was higher than 80%, and that for cracking products was less than 15%. At 773 K cracking selectivity increased and hydrogen transfer selectivity decreased but still was the dominant reaction.

Experimental conversion plots at different times on stream and reaction temperatures are shown in Figs. 1a and 1b. In all cases conversion decreases progressively as time on stream increases, because of catalyst decay.

When conversions are compared under the same reaction conditions, it may be observed that 1-octene yields the highest values, followed by decalin and tetralin. For instance, at a reaction temperature of 673 K and a time on stream of 5 s, 1-octene conversion was 94 wt%, and decalin and tetralin conversions were 50 and 16 wt%, respectively. 1-Octene also

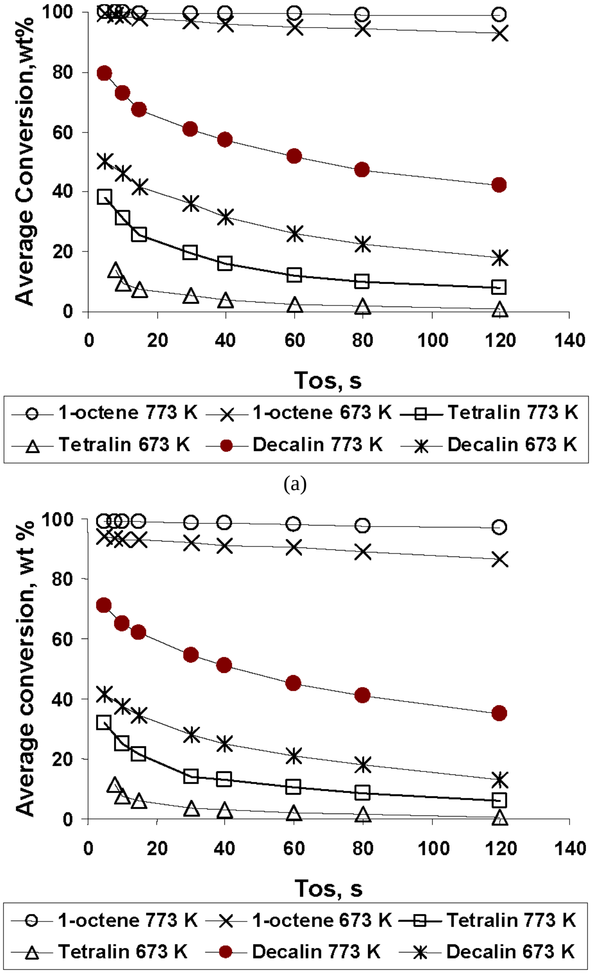

(a)

(b)

Fig. 1. (a) Experimental conversion feed flow = 3 g/min. (b) Experimental conversion feed flow = 4 g/min.

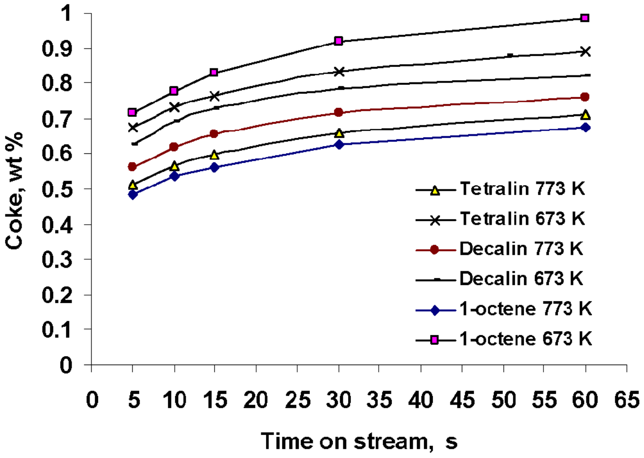

Fig. 2. Coke on spent catalyst.

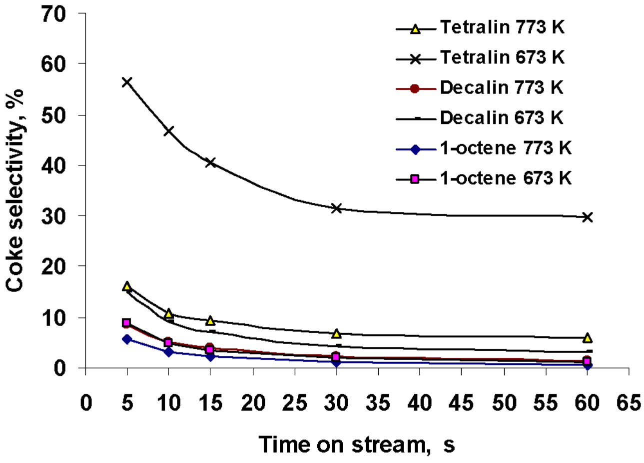

Fig. 3. Core selectivity.

shows the lowest conversion drop when the time on stream is increased or the reaction temperature is decreased. Thus the reactivity order is as follows: 1-octene > decalin > tetralin.

The high reactivity of 1-octene may be explained by the presence of the double bond, which can be easily protonated by the Brønsted sites of the catalyst. The low reactivity of tetralin is explained by the stabilizing effect of the resonating structure of the aromatic part of this molecule and the fact that only five single carbon–carbon bonds of the naphthenic ring are able to react.

It is widely accepted that coke is responsible for catalyst decay; however, our results indicate that catalyst decay does not correlate well with coke deposited on the catalyst. For instance, even though 1-octene yields the highest coke formation at 673 K (Fig. 2), the conversion drop observed is the lowest (Figs. 1a and 1b). In contrast, tetralin gives the highest conversion drop but does not form the most coke on the catalyst. Furthermore, in all cases coke builds up very fast on the catalyst surface during the first instants of the reaction; about 70% of the total coke built up during 60 s is formed within the first 5 s. However, conversion does not decrease in a corresponding proportion, indicating that other factors besides coke formation may influence catalyst decay. Moreover, as illustrated in Fig. 3, coke selectivity is higher at lower temperatures and depends on the chemical nature of the reactant; tetralin shows the highest coke selectivity, followed by decalin and 1-octene. At 673 K and 5 s, coke selectivity is about 55%, and it is importantly reduced to 29% at 773 K. Likewise, in all cases coke selectivity decreased very fast as time on stream increased.

All of these observations can be explained by differences in adsorption, as will be shown below.

3.1. Kinetic parameters

When experimental data were fitted to a pseudo-homogeneous model (Eq. (2)), good fittings were obtained, regardless of the reactant (Figs. 4–6). The kinetic rate constants obtained with the pseudo-homogeneous model are listed in Table 4; they are consistent with the ranking of reactivity described above, 1-octene > *n*-hexadecane > decalin > tetralin. The kinetics of *n*-hexadecane was reported in a previous paper [20].

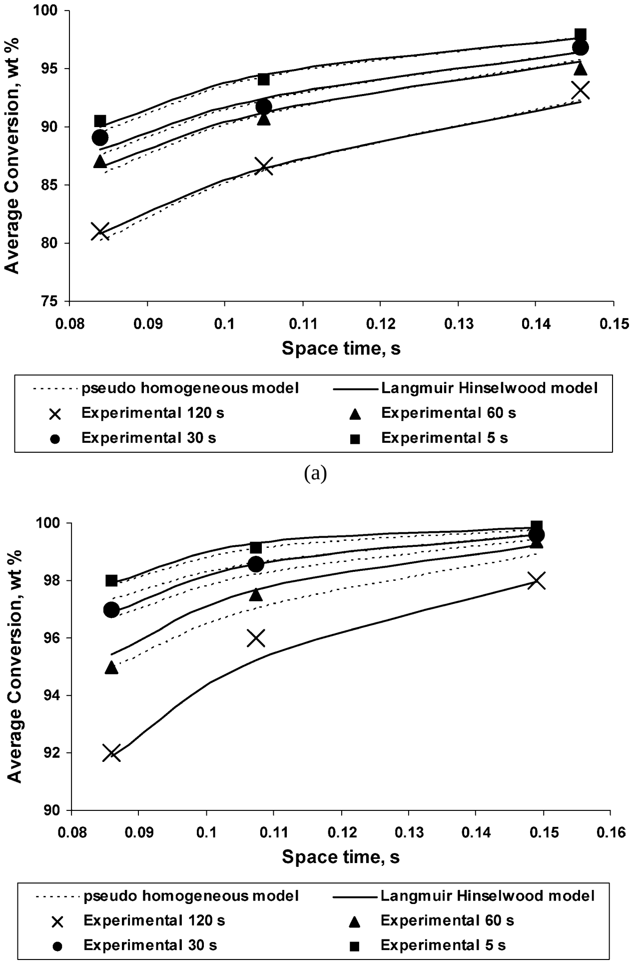

(a)

(b)

Fig. 4. (a) 1-Octene kinetics at 673 K. (b) 1-Octene kinetics at 773 K.

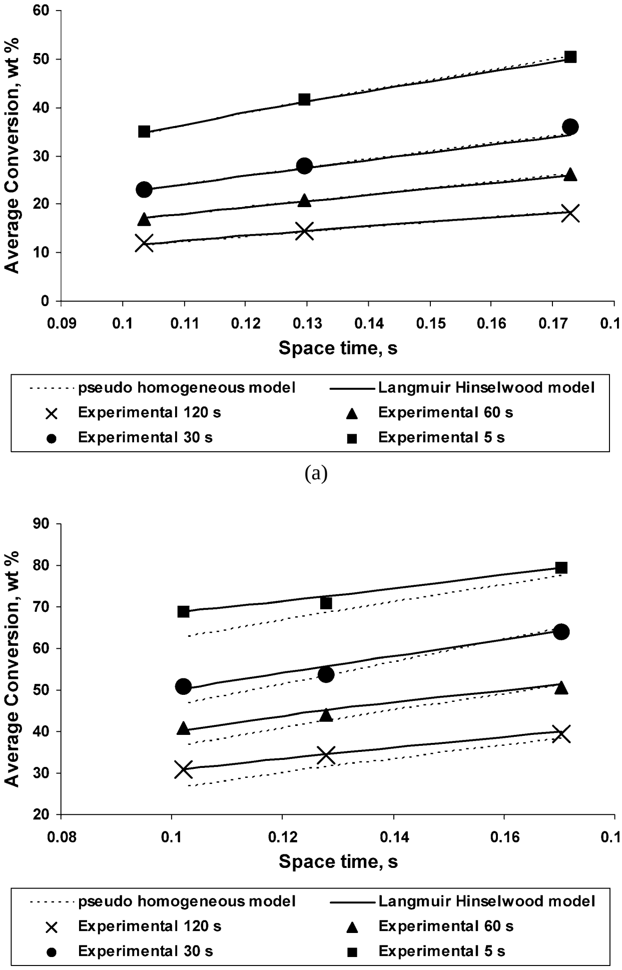

(a)

(b)

Fig. 5. (a) Decalin kinetics at 673 K. (b) Decalin kinetics at 773 K.

Catalyst decay constants show an inverse order in which the highest and lowest values corresponded to tetralin and 1-octene, respectively. When reaction temperature was increased, the decay constants decreased, indicating that they could include other parameters besides the kinetic decay constant. Moreover, when the activation energies are considered, it can be seen that the lowest value corresponds to tetralin, whose reactivity is the lowest; likewise, activation energies obtained for 1-octene and *n*-hexadecane are equivalent, even though 1-octene is much more reactive than *n*-hexadecane. These inconsistencies call into question the validity of the pseudo-homogeneous kinetic model.

When the Langmuir–Hinselwood model, which takes into account the adsorption effects of reactants and products, is considered (Eq. (3)), the fitting is very good (Figs. 4–6). In this case the sum of the squares of residuals is smaller than when the pseudo-homogeneous model is used; what is not surprising is that the number of parameters is larger in Eq. (3) than in Eq. (2). The kinetic parameters are listed in Table 5.

Haag et al. [5] have shown that activation energy for cracking is the sum of the heat of adsorption plus the intrinsic activation energy. Thus even though the apparent activation energies for tetralin, decalin, and *n*-hexadecane are similar, the true activation energies show significant differences, which are in line with the experimental reactivities observed, that is, the lowest activation energy and the highest reactivity correspond to 1-octene, and the highest activation energy observed is that for tetralin, which demonstrates the lowest reactivity. The high activation energies obtained for tetralin (357 kJ/mol), *n*-hexadecane (349 kJ/mol), and decalin (319 kJ/mol) may be an indication that they are mainly transformed by a protolytic cracking mechanism, whereas 1-octene will follow a β-scission type cracking with a lower true activation energy (256 kJ/mol).

Regarding the adsorption constants of reactants, tetralin shows the highest values, followed by *n*-hexadecane, decalin, and 1-octene; adsorption constants decrease with increasing reaction temperature, as should be the case for exothermic processes.

Adsorption heats were derived from the calculated adsorption constants using the Van't Hoff equation. The highest value was obtained for tetralin (153 kJ/mol), followed by 1-octene (115 kJ/mol), *n*-hexadecane (137 kJ/mol),

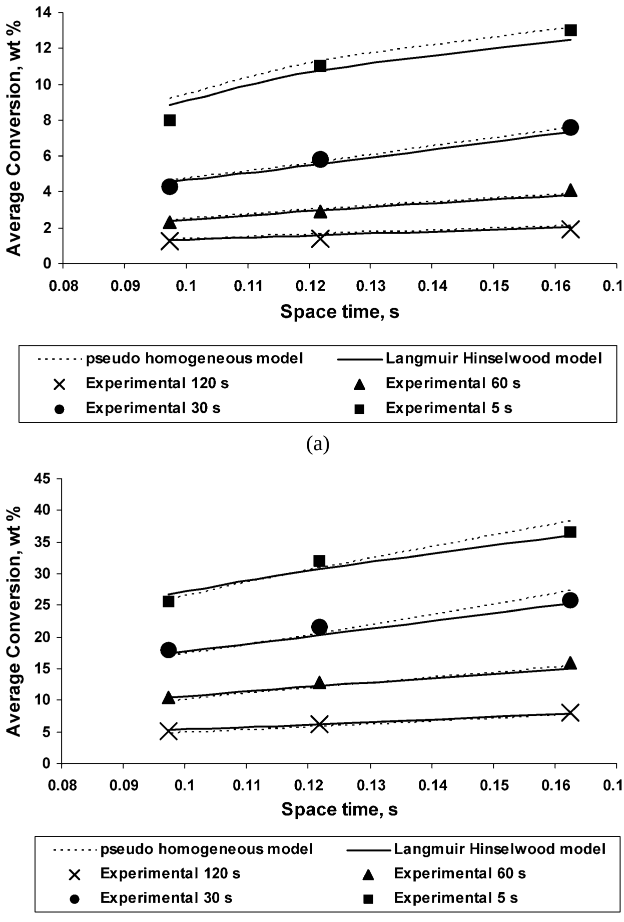

(a)

(b)

Fig. 6. (a) Tetralin kinetics at 673 K. (b) Tetralin kinetics at 773 K.

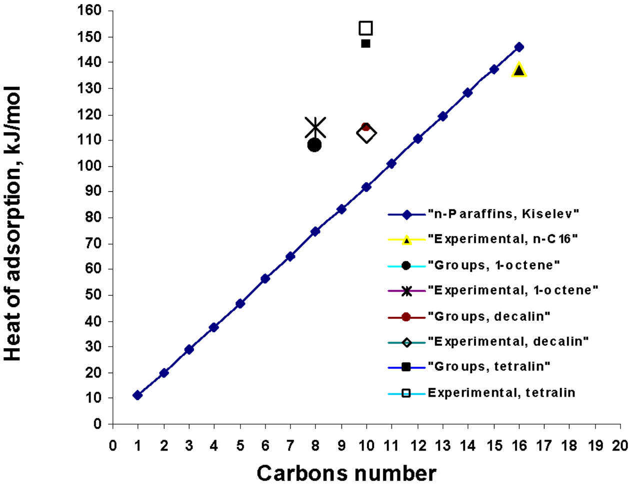

Fig. 7. Heats of adsorption.

and decalin (113 kJ/mol). These values compare well with those calculated by group contribution [21] for tetralin (147 kJ/mol), 1-octene (109 kJ/mol), and decalin (115 kJ/mol) and with the data reported by Kiselev [1] for n-hexadecane (146 kJ/mol). This order appears to be consistent with the interactions expected according to the chemical nature of these compounds and the surface of the catalyst. Kiselev et al., who used a Y zeolite, and Bokhoven et al. [13], who used a mordenite, reported that the heat of adsorption of n-alkanes over zeolites increases linearly with the chain length of the hydrocarbon, indicating that the heat of adsorption is due to the van der Waals interactions of the hydrocarbon with the surface of the zeolite. The value we obtained for n-hexadecane is in line with this, as can be seen in Fig. 7. For decalin, a value close to that reported for n-decane could be expected, since both molecules are saturated hydrocarbons with the same number of carbon atoms. However, we have obtained kinetically a higher value for decalin than for n-decane; the heat of adsorption of decalin is similar to that of n-dodecane, which has the same number of carbon–carbon bonds. The heat of adsorption of 1-octene is clearly higher than that of n-octane; the obvious reason for this is the presence of the double bond of 1-octene, which strongly interacts with the Brønsted sites of the catalyst, giving the corresponding alkoxide. Tetralin shows the highest adsorption heat, 60 kJ/mol higher than the n-paraffin with the same number of carbon atoms and 40 kJ/mol higher than decalin. The reason for this should be related to the three conjugated double bonds in the aromatic ring. Adsorption not only influences the relative rate of the reaction, as

Table 4
Kinetic parameters according to the pseudohomogeneous model

	$\sum Kr$ (s^{-1})		Kd (s^{-1})		$\sum$(residuals)^2		Activation energy (kJ/mol)
Temp. (K)	673	773	673	773	673	773	
n-Hexadecane	4.7	8.2	0.47	0.065	0.0018	0.0023	24.1
Decalin	5.02	13.06	0.076	0.069	0.0003	0.0048	41.4
Tetralin	3.72	5.72	1.63	0.327	0.0001	0.0003	18.6
1-Octene	33.85	60.13	0.0091	0.0049	0.0020	0.0030	24.9

Table 5
Kinetic parameters according to the Langmuir–Hinselwood model

	$\sum Kr$ (s^{-1})		K_A (l/mol)		$\sum Kp_in_i$ (l/mol)		Kd (s^{-1})		$\sum$(residuals)^2		Adsorption heat (kJ/mol)	Apparent activation energy (kJ/mol)	True activation energy (kJ/mol)
Temp. (K)	673	773	673	773	673	773	673	773	673	773			
n-Hexadecane	8.6	1147	2.31	0.096	51	16	2.200	2.100	0.0009	0.0006	−137.6	211.7	349.3
Decalin	3.69	431	1.48	0.109	13.6	190	0.081	0.144	0.0002	0.0008	−112.9	206.0	318.9
Tetralin	0.577	64.84	7.15	0.208	40	170	1.610	0.690	0.0001	0.0002	−153.1	204.3	357.4
1-Octene	117.3	3118	0.36	0.025	12.93	0.928	0.010	0.005	0.0004	0.0017	−115.0	141.9	256.9

discussed above, but may also have an important impact on catalyst deactivation.

3.2. *Adsorption and catalyst decay*

The importance of adsorption on catalyst decay can be inferred from the fact that, as occurs with adsorption constants, catalyst decay constants also decrease with increasing reaction temperature, as can be seen in Tables 4 and 5. Adsorption of reactants and products can play an important role in catalyst decay, as when the strong adsorption of basic nitrogenated hydrocarbons on the Brønsted sites of the zeolite reduces its activity.

An examination of the reaction products of each of the reactants tested (Tables 2 and 3) indicates that 1-octene is the reactant that produces the lowest yields of aromatics and heavier hydrocarbons, whereas tetralin produces de highest yields. Since we have seen that tetralin, because of the presence of the aromatic ring, has the highest adsorption constant and heat of adsorption among the reactants studied, it can be expected that reaction products formed from tetralin, such as di-aromatic naphthalene, methyl naphthalene, and heavier aromatics, should strongly compete for adsorption, reducing the active sites available for cracking and consequently reducing the reaction rate. At 773 K adsorption constants are lower, and, in consequence, coke yield and catalyst deactivation by competitive adsorption are also lower. Similar observations have been reported by Forissier [22] and Nevicato [23].

Decalin also produces tetralin, di-aromatics, and heavier aromatics, but to a lower extent than tetralin; therefore the catalyst decay constants are lower. In the case of 1-octene the catalyst decay constants are very low, and, even though it yields at least the same amount of coke as tetralin or decalin, its deactivation rate is much lower. This is explained by the fact that 1-octene does not produce large amounts of di-aromatics or heavy aromatics, whose adsorption on the catalyst surface contributes to catalyst deactivation, as occurred during cracking of tetralin or decalin.

Thus catalyst deactivation is explained not only by coke deposited on catalyst and pore plugging; reactants and products adsorption may also play an important role, which is especially important for the cracking of heavy feeds. To test this hypothesis, we have carried out some experiments in which the activity of the catalyst was measured in three different scenarios under constant operating conditions and according to the procedure described in the Experimental section. In one scenario we used the fresh catalyst in order to have a basis for comparison. In another, we used the coked catalyst, which was obtained after the reaction and stripping steps. Finally, in the third scenario we used the coked and unstripped catalyst obtained after the reaction step. The corresponding results are listed in Table 6, in which it can be seen that if adsorbed hydrocarbons on spent catalyst are properly stripped by N_2 and the catalyst is exposed to a new reaction without elimination of the coke deposited on its surface, it preserves an activity that is up to 93% of the base. In contrast, when experiments were carried out with the omission of the stripping step, leaving the adsorbed hydrocarbons on the catalyst, the remaining catalytic activity was only about 20% of the base, showing the important role of the adsorbed products (not removed by stripping) on catalyst decay [24–27]. It should be pointed out that for these experiments we used a vacuum gasoil to ensure that the catalyst surface was completely covered by coke.

Table 6
Effect of adsorbed hydrocarbons on catalyst activity

	Base	Catalyst	
		Stripped and coked	Unstripped and coked
Coke on catalyst (wt%)	0	1.9	2.1
Conversion (wt%)	91.4	85.6	18.3
Yields (wt%)			
Dry gas	2.1	3.4	1.8
Propane	3.4	2.9	0.7
Propylene	7.9	7.1	2.3
Butanes	3.2	2.6	0.9
Butylenes	5.9	5.2	1.5
Gasoline	49.8	45.8	3.5
Cyclic oil	12.3	17.9	6.5
Resid	8.6	14.4	81.7
Coke	6.8	0.6	1
Operating conditions			
Catalyst weight (g)		3	
Reaction temperature (K)		783	
Time on stream (s)		30	
Catalyst to oil ratio		4	
Feed properties			
Specific gravity		0.91	
Inicial boiling point (K)		623	
Final boiling point (K)		813	
Carbon Conradson (wt%)		0.4	

On the other hand, for the cracking of gasoil the picture is more complex, not only for the large number of chemical species involved in the process, but also because of the lack of knowledge of its adsorption effects. However, the knowledge acquired from cracking pure components may provide some useful guidance. According to the results reported here, it can be inferred that aromatic gasoils will render lower conversions than naphthenic and paraffinic gasoils, because of the lower reaction rate constants and the higher adsorption constants, which in turn will promote a faster catalyst deactivation.

Gasoil cracking may be improved by operation at higher temperature, not only because of the endothermicity of the reaction, but also because of the lower adsorption constant of undesirable hydrocarbons, such as aromatic compounds, which are refractory to cracking, or basic hydrocarbons, which may occupy the catalyst acid sites. The lower adsorption rate also will promote a better catalyst stripping and a lower coke yield. This may promote a higher flexibility in the operation of the unit. The limit, of course, will be set by the thermal cracking and the metallurgy of the FCC unit.

4. Conclusions

It is possible to obtain adsorption constants under cracking reaction conditions from kinetics with Langmuir–Hinselwood models.

The heat of adsorption for paraffins and naphthenes corresponds to the physical heat due to van der Waals interactions between the hydrocarbon and the zeolite walls, in agreement with previous adsorption work [1,13]. Naphthene (decalin) heat of adsorption corresponds approximately to that of a paraffin with the same number of carbon–carbon bonds, and the presence of the double bond in an olefin increases the heat of adsorption by $\sim 40\ \text{kJ}/(\text{mol mol})$ compared with the corresponding paraffin. A similar difference in adsorption constant was observed for a comparison of heats of adsorption of decalin and tetralin, which is due to the presence of an aromatic ring. These differences in heat of adsorption are not only responsible for differences in the apparent activation energies, but also have an important impact on catalyst deactivation.

Acknowledgments

The authors thank CICYT for financial support (project MAT2003-07945-C02-01). F.J.O. tanks IMP for financial support.

References

[1] V. Kiselev, Adv. Chem. 102 (1971) 37.
[2] T.F. Narbeshuber, H. Vinek, J. Lercher, J. Catal. 157 (1995) 388–395.
[3] S.M. Babitz, B.A. Williams, J.T. Miller, R.Q. Snurr, W.O. Haag, H.H. Kung, Appl. Catal. A 179 (1999) 71–86.
[4] J.A. Bokhoven, M. Tromp, D.C. Koningsberger, J.T. Miller, J.A.Z. Pieterse, J.A. Lercher, B.A. Williams, H.H. Kung, J. Catal. 202 (2001) 129–140.
[5] W.O. Haag, R.M. Dessau, R.M. Lago, Chemistry of Microporous Materials, Stud. Surf. Sci. Catal., vol. 60, Elsevier, Amsterdam, 1991, p. 255.
[6] N. Arsenova-Härtel, H. Bludau, R. Schumacher, W.O. Haag, H.G. Karge, E. Brunner, U. Wild, J. Catal. 191 (2000) 326.
[7] N. Arsenova, H. Bludau, W.O. Haag, H.G. Karge, Micropor. Mesopor. Mater. 23 (1998) 1.
[8] F. Eder, J.A. Lercher, Zeolites 18 (1997) 75.
[9] J.E. Rekoske, R.J. Madon, L.M. Aparicio, J.A. Dumesic, Stud. Surf. Sci. Catal. 75 (1993) 1563, part B.
[10] J. Pruski, A. Pekediz, H. de Lasa, Chem. Eng. Sci. 51 (1996) 1799.
[11] A. Gianetto, H.I. Farag, A.P. Blasetti, H. de Lasa, Ind. Eng. Chem. Res. 33 (1994) 3053.
[12] Y. Zhao, B.W. Wojciechowski, J. Catal. 142 (1993) 499.
[13] J.A. van Bokhoven, B.A. Williams, W. Ji, D.C. Koningsberger, H.H. Kung, J.T. Miller, J. Catal. 224 (2004) 50–59.
[14] A. Corma, J. Martínez-Triguero, C. Martínez, J. Catal. 197 (2001) 151.
[15] M. Grzesik, J. Skrzypek, B.W. Wojciechowski, Chem. Eng. Sci. 48 (1993) 3273.
[16] M.R. Viner, B.W. Wojciechowski, Can. J. Chem. Eng. 60 (1982) 127.
[17] G. Buzzi, Ing. Chim. Ital. 4 (12) (1968) 171.
[18] A. Corma, V. González-Alfaro, A.V. Orchillés, J. Catal. 200 (2001) 34.
[19] M.A. Sánchez-Castillo, R.J. Madon, J.A. Dumesic, J. Phys. Chem. B 109 (2005) 2164.
[20] A. Corma, O. Marie, F.J. Ortega, J. Catal. 222 (2004) 338.
[21] W. Schirmer, Chem. Techn. 23 (2) (1971) 98.
[22] M. Forissier, J.R. Bernard, in: C.H. Bartholomew, J.B. Butt (Eds.), Catalyst Deactivation, Elsevier, Amsterdam, 1991, p. 359.
[23] D. Nevicato, I. Pitault, M. Forissier, J.R. Bernard, in: B. Delmon, G.F. Froment (Eds.), Catalyst Deactivation, Elsevier, Amsterdam, 1994, p. 249.
[24] R. Hughes, G. Hutchings, C.L. Koon, B. McGhee, C.E. Snape, Stud. Surf. Sci. Catal. 88 (1994) 377.
[25] J. Pruski, A. Pekediz, H. de Lasa, Chem. Eng. Sci. 51 (1996) 1749.
[26] C. Delattre, M. Forissier, I. Pitault, D. Schweich, J.R. Bernard, Chem. Eng. Sci. 56 (2001) 1337.
[27] S. Chen, G. Manos, Catal. Lett. 3 (2004) 195.